KURENAI
Kyoto University Research Information Repository

KYOTO UNIVERSITY

Title	Structural and mutational analysis of amino acid residues involved in ATP specificity of Escherichia coli acetate kinase.
Author(s)	Yoshioka, Aya; Murata, Kousaku; Kawai, Shigeyuki
Citation	Journal of bioscience and bioengineering (2014), 118(5): 502-507
Issue Date	2014-05-23
URL	http://hdl.handle.net/2433/198558
Right	© 2014 The Society for Biotechnology, Japan. Published by Elsevier B.V. Licensed under the Creative Commons Attribution-NonCommercial-NoDerivatives 4.0 International http://creativecommons.org/licenses/by-nc-nd/4.0/. NOTICE: this is the author's version of a work that was accepted for publication in Journal of Bioscience and Bioengineering. Changes resulting from the publishing process, such as peer review, editing, corrections, structural formatting, and other quality control mechanisms may not be reflected in this document. Changes may have been made to this work since it was submitted for publication. A definitive version was subsequently published in Journal of Bioscience and Bioengineering, Volume 118, Issue 5, Pages 502–507. doi:10.1016/j.jbiosc.2014.04.014.
Type	Journal Article
Textversion	author

1   Title: Structural and mutational analysis of amino acid residues involved in ATP

2   specificity of *E. coli* acetate kinase

3

4   Short title: Specificity to ATP of acetate kinase

5

6   Author names: Aya Yoshioka, Kousaku Murata, Shigeyuki Kawai [*]

7

8   Affiliations: Laboratory of Basic and Applied Molecular Biotechnology, Division

9   of Food Science and Biotechnology, Graduate School of Agriculture, Kyoto

10   University, Uji, Kyoto 611-0011, Japan

11

12   [*]To whom correspondence should be addressed.

13   Tel: +81 774 38 3768; Fax: +81 774 38 3767; E-mail: kawais@kais.kyoto-u.ac.jp.

14

15

16

17

18 **Abstract**

19 Acetate kinase (AK) generally utilizes ATP as a phosphoryl donor, but AK

20 from *Entamoeba histolytica* (PPi-ehiAK) uses PPi, not ATP, and is PPi-specific.

21 The determinants of the phosphoryl donor specificity are unknown. Here, we

22 inferred 5 candidate amino acid residues associated with this specificity, based on

23 structural information. Each candidate residue in *Escherichia coli* ATP-specific

24 AK (ATP-ecoAK), which is unable to use PPi, was substituted with the respective

25 PPi-ehiAK amino acid residue. Each variant ATP-ecoAK had an increased K_m for

26 ATP, indicating that the 5 residues are the determinants for the specificity to ATP

27 in ATP-ecoAK. Moreover, Asn-337 of ATP-ecoAK was shown to be particularly

28 significant for the specificity to ATP. The 5 residues are highly conserved in 2,625

29 PPi-ehiAK homologs, implying that almost all organisms have ATP-dependent,

30 rather than PPi-dependent, AK.

31

34

35

Introduction

Acetate kinase (AK) is a critical enzyme for central carbon metabolism in bacteria and archea (1). ATP-dependent AK catalyzes the phosphorylation of acetate to produce acetyl phosphate by utilizing ATP as a phosphoryl donor and also catalyzes the reverse reaction (2). This enzyme has been purified and characterized from various archaea and bacteria, including *Methanosarcina thermophila*, *Escherichia coli, Thermotoga maritima*, and *Lactobacillus sanfranciscensis* (3-7). The three-dimensional structure of AK of *M. thermophila* (mthAK) has been solved (8) and several key catalytic residues have been identified based on the tertiary structural information and site-directed mutagenesis (8-15).

Flower et al. have recently shown that the AK of the amitochondriate protist *Entamoeba histolytica* (PPi-ehiAK) is a novel PPi-dependent AK that phosphorylates acetate using PPi, not ATP, as a phosphoryl donor (16). The three-dimensional structure of PPi-ehiAK has been solved and the substrate-binding site of PPi-ehiAK has been compared with that of mthAK, although without a biochemical verification (17). Despite the differences in phosphoryl donor specificity, the primary sequences of AK enzymes are highly conserved (8, 17).

The significance of AK in central carbon and energy metabolism indicates the importance of understanding the determinants of the specificity of AK for phosphoryl donors (ATP and PPi). Such understanding is also important in a structural biology context, given the structural overlap between ATP and PPi (Fig. 1). In this study, we verified that PPi-ehiAK is specific for PPi, and does not

60   accept ATP; and that *E. coli* AK (ATP-ecoAK) is specific for ATP, and not for PPi.

61   We then identified the amino acid determinants of the specificity to ATP of

62   ATP-ecoAK based on a comparison of the tertiary structures of mthAK and

63   PPi-ehiAK and the primary structures of mthAK, PPi-ehiAK, and ATP-ecoAK,

64   combined with site-directed mutagenesis of ATP-ecoAK.

65

66   **MATERIALS AND METHODS**

67

68   **Expression of PPi-ehiAK**   *PPi-ehiAK* (KEGG ID, ehi, EHI_170010) with

69   optimized codon usage for *E. coli* was synthesized at Operon (Tokyo, Japan)

70   (Supplementary Fig. S1). *PPi-ehiAK* was amplified by PCR using the synthesized

71   gene as a template with primers AK_pQE_B_F (5´-TCA CCA TCA C<u>GG ATC</u>

72   <u>C</u>AT GTC TAA TGT GCT GAT TTT C-3´, with the *Bam*HI site underlined) and

73   AK_pQE_S_R (5´-GCT GCA GGT CGA CCC TTA AAA CTG GAA TAA TTC

74   TTT C-3´). The PCR product was inserted into *Bam*HI/*Sma*I sites in pQE-80L

75   with In-Fusion (Clontech, Otsu, Japan), yielding pMK3549. *E. coli* MK3648

76   strain was obtained by transforming *E. coli* NovaBlue (Novagen) with pMK3549

77   and plasmid pLysSRARE (Novagen). PPi-ehiAK is expressed as a N-terminally

78   His-tagged protein in *E. coli* MK3648.

79   For expression of PPi-ehiAK, a fresh single colony of MK3648 strain that had

80   just been transformed was inoculated into 10 mL LB medium supplemented with

81   100 µg/mL ampicillin, 34 µg/mL chloramphenicol, and 12.5 µg/mL tetracycline.

82   After culturing at 37°C aerobically overnight, the culture was transferred to the

83   same medium (250 mL) and cultured at 37°C aerobically overnight. This culture

4

84   was again transferred to the same medium (4.5 L, 500 mL in a 2.0 L Sakaguchi

85   flask) and cultivation was continued at 37°C aerobically until A_{600} reached 0.4.

86   Then, isopropyl-1-β-D-thiogalactopyranoside was added to 1 mM and cultivation

87   was continued further at 37°C aerobically for 1 h.

88

89   **Purification of PPi-ehiAK**   MK3648 cells overexpressing PPi-ehiAK were

90   collected by centrifugation at 8,500 g for 10 min, suspended in 50 mL of 20 mM

91   HEPES-NaOH (pH 7.5), and disrupted by sonication at 4°C for 15 min with an

92   Insonator 201M (Kubota, Tokyo, Japan). After centrifugation at 20,000 g for 10

93   min, the clear supernatant was used as the cell extract containing PPi-ehiAK. This

94   cell extract was applied to a Talon Metal Affinity Resin column (2.5×4.5 cm)

95   (Clontech) equilibrated with 20 mM HEPES-NaOH (pH 7.5). After washing with

96   150 mL of 20 mM HEPES-NaOH (pH 7.5) containing 30 mM imidazole and 300

97   mM NaCl, PPi-ehiAK was eluted with 150 mL of 20 mM HEPES-NaOH (pH 7.5)

98   containing 150 mM imidazole and 300 mM NaCl. The fractions containing

99   PPi-ehiAK were combined, dialyzed against 20 mM HEPES-NaOH (pH 7.5) at

100   4°C overnight, and used as the purified PPi-ehiAK. If necessary, the purified

101   enzyme was concentrated by 3-fold with a Centriprep 10K instrument (Millipore).

102

103   **Expression of ATP-ecoA**   For expression of ATP-ecoAK (KEGG ID, ecj,

104   Y75_p2262), *E. coli* K12 AG1 ASKA GFP-free strain (MK3814 strain), which

105   contained plasmid pMK3814 (pCA24N carrying the *ATP-ecoAK* gene without

106   GFP) (18) and was stored at -80°C in the presence of 17% v/v glycerol, was

107   inoculated into 20 mL LB medium supplemented with 34 µg/mL chloramphenicol

108   and cultured at 37°C aerobically overnight. This culture was transferred to the

109   same medium (700 mL, 350 mL in a 500 mL Sakaguchi flask) and cultivation was

110   continued at 37°C aerobically until A_{600} reached 0.6. Then,

111   isopropyl-1-β-D-thiogalactopyranoside was added to 0.1 mM and cultivation was

112   continued at 37°C aerobically for 3 h. Purification and dialysis were conducted as

113   described for PPi-ehiAK above, but with use of 10 mM Tris-HCl (pH 8.0) instead

114   of 20 mM HEPES-NaOH (pH 7.5).

115

116   **Expression of variant ATP-ecoAK**   Site-directed mutagenesis was performed

117   using inverse PCR followed by *Dpn*I treatment using pMK3814 as a template.

118   The variant ATP-ecoAK plasmids were confirmed by DNA sequencing. These

119   plasmids were introduced into the *E. coli* DH5α strain and each variant

120   ATP-ecoAK was expressed and purified as described below for ATP-ecoAK.

121

122   **Assay of AK activity**   The AK activity in the acetyl phosphate-forming

123   direction was assayed at 30°C using a hydroxamate assay that detects formation of

124   acetyl phosphate (2, 19). The assay utilizes the reaction of acetyl phosphate with

125   hydroxylamine to form acetyl hydroxamate, which forms a colored complex with

126   trivalent iron. The reaction mixture (333 µL) comprised 10 mM phosphoryl donor,

127   150 mM HEPES-NaOH (pH 6.5), 200 mM potassium acetate, 10 mM $MgCl_2$, 700

128   mM hydroxylamine hydrochloride, with the pH adjusted to pH 6.5 with KOH just

129   before use, and an appropriate amount of AK. The reaction was initiated by

130   addition of AK and terminated by addition of 333 µL of 10% trichloroacetic acid,

131   followed by addition of 333 µL of 2.5% $FeCl_3$ in 2.0 N HCl. After incubation for

6

132   5 min, the absorbance at 540 nm (A_{540}) was measured and defined as [1]A_{540}. PPi

133   (Nakalai Tesque, Kyoto, Japan) and ATP (Wako Pure Chemical) were used as

134   phosphoryl donors. AK was diluted with 20 mM HEPES-NaOH (pH 7.5) or 10

135   mM Tris-HCl (pH 8.0) if required. Control reactions were conducted without a

136   phosphoryl donor and the resultant A_{540} was defined as [2]A_{540}. AK activity was

137   calculated as ΔA_{540} ([1]A_{540} - [2]A_{540}).

138   The AK activity in the PPi-forming direction was assayed at 30°C by detecting

139   formation of PPi using a PPiLight[TM] inorganic pyrophosphate assay (Lonza, Basel,

140   Switzerland) (20, 21). This assay utilizes the reactions of PPi with AMP to form

141   ATP, and of luciferase producing light from the newly formed ATP. The reaction

142   mixture (50 µL) comprised 100 mM HEPES-NaOH (pH 6.5), 20 mM potassium

143   phosphate (Pi) (pH 7.0), 20 mM $MgCl_2$, 1.5 mM acetyl phosphate, and an

144   appropriate amount of AK. The reaction was initiated by addition of AK and

145   terminated by boiling for 5 min. After the reaction, 20 µL of PPiLight[TM]

146   Converting Reagent was added to the reaction mixture (40 µL) with appropriate

147   dilution with distilled water (e.g., 50-fold dilution for the PPi-ehiAK reaction).

148   After incubation at room temperature for 30 min, 20 µL of PPiLight[TM] Detection

149   Reagent was added and the mixture (60 µL) was further incubated at room

150   temperature for 30 min. Luminescence of the mixture was then read with a 0.1 s

151   integration time and the relative luminescent unit (RLU) value was measured as

152   [1]RLU. Control reactions were conducted without AK and the resultant RLU was

153   defined as [2]RLU. AK activity in the PPi-forming direction was calculated as

154   ΔRLU ([1]RLU – [2]RLU) using an authentic PPi as a standard.

155   One unit (U) of enzyme activity was defined as 1 µmol acetyl phosphate

156 produced in 1 min at 30°C and specific activity was expressed in U/mg protein.

157 Protein concentrations were determined by the method of Bradford (22) with

158 bovine serum albumin as a standard.

159

160 **Differential scanning fluorimetry (DSF)**   Interaction between AK and

161 substrate (ATP or PPi) was assessed by DSF (23) using a MyiQ2 real-time PCR

162 instrument (Bio-Rad). The fluorescence of SYPRO Orange (Invitrogen) was

163 monitored using filters provided with the PCR instrument (excitation at 492 nm

164 and emission at 610 nm). The reaction mixture (20 µl) comprised 5 µg AK, 20

165 mM Tris-HCl (pH 7.5), 1000-fold diluted SYPRO Orange, and each substrate (1.0

166 mM ATP, 5.0 mM PPi). This mixture was subjected to a temperature increase

167 from 20 to 95°C by 0.5°C/cycle for a total of 141 cycles. The fluorescence profile

168 was obtained by plotting the relative fluorescence unit (RFU) value at each

169 temperature. The profile was analyzed using *iQ5* (Bio-Rad) and the midpoint of

170 the increase in the profile was defined as the melting temperature (T_m).

171

172 **Elution of AKs from an ATP-agarose column**   Purified ATP-ecoAK in 10

173 mM Tris-HCl (pH 8.0) containing 10 mM $MgCl_2$ (500 µL, 1.0 mg/mL) was

174 applied to an ATP-agarose column (100 µL) (Sigma-Aldrich) equilibrated with 10

175 mM Tris-HCl (pH 8.0) containing 10 mM $MgCl_2$. The column was allowed to

176 stand for 1 h at 4°C for binding to take place. After incubation, the column was

177 washed with 2 mL of 10 mM Tris-HCl (pH 8.0) containing 10 mM $MgCl_2$. Next,

178 500 µL of 50 mM ATP (pH 7.0) containing 10 mM $MgCl_2$ was added and the

179 column was incubated for 30 min at 4°C, followed by elution of ATP-ecoAK. In

180 the case of purified PPi-ehiAK in 20 mM HEPES-NaOH (pH 7.5) containing 10

181 mM MgCl$_2$ (500 µL, 1.0 mg/mL), the application, washing, and elution

182 procedures were the same as those for ATP-ecoAK, but with use of 20 mM

183 HEPES-NaOH (pH 7.5) instead of 10 mM Tris-HCl (pH 8.0).

184

185 **SDS-PAGE**   SDS-PAGE was performed on 12.5% acrylamide gels.(24)

186 Proteins in the gel were visualized with Coomassie brilliant blue R-250.

187

188 **RESULTS**

189

190 **Purification and phosphoryl donor specificity of PPi-ehiAK and**

191 **ATP-ecoAK**   An *PPi-ehiAK* gene with optimized codon usage for *E. coli* was

192 synthesized (Fig. S1), cloned in pQE-80L, and expressed as a N-terminally

193 His-tagged protein in *E. coli*. The purified PPi-ehiAK protein was 44 kDa on

194 SDS-PAGE, in agreement with the calculated molecular mass (44 kDa; His-tag, 1

195 kDa + PPi-ehiAK, 43 kDa) (Fig. S2). Kinetic constants showed that the purified

196 PPi-ehiAK utilized PPi, but not ATP, as a phosphoryl donor (Table 1). Native

197 ATP-ecoAK purified from *E. coli* utilizes ATP (7), but the strict phosphoryl donor

198 specificity of ATP-ecoAK is unknown. To examine this issue, a N-terminally

199 His-tagged ATP-ecoAK was also expressed in *E. coli*. The purified ATP-ecoAK

200 was shown to be specific for ATP, and not to use PPi as a phosphoryl donor (Table

201 1).

202

203 **Candidates for determinants of the phosphoryl donor specificity of AK**

204   To probe the structural determinants of the phosphoryl donor specificity of AK,

205   we inspected the substrate-binding site of the tertiary structure of mthAK

206   complexed with acetate and ADP-AlF$_3$ (9). Noted that although mthAK utilizes

207   ATP for the phosphorylation of acetate (5), if mthAK uses PPi or not has not been

208   experimentally confirmed. We found 12 residues located within 4.0 Å of ADP:

209   Leu-209, Gly-210, Asn-211, Asp-283, Phe-284, Arg-285, Ala-330, Gly-331,

210   Ile-332, Asn-335, Ser-336, and Arg-362. Among these residues, 5 (Asn-211,

211   Ala-330, Gly-331, Ile-332, and Asn-335 of mthAK) are conserved in ATP-ecoAK,

212   but not in PPi-ehiAK, based on a multiple sequence alignment (Fig. 2). This

213   suggests that these residues are candidates for determinants of the phosphoryl

214   donor specificity. Four of these 5 residues (Asn-211, Gly-331, Ile-332, and

215   Asn-335) form hydrogen bonds and van der Waals contacts to ADP (Table S1). Of

216   the other 7 residues among the original 12 in mthAK, two (Ser-336 and Arg-362)

217   are not conserved and 5 (Leu-209, Gly-210, Asp-283, Phe-284, and Arg-285) have

218   defined roles (8, 12) and are conserved in both ATP-ecoAK and PPi-ehiAK (Fig.

219   2).

220   Among the 5 candidate residues, Asn-211, Gly-331, and Ile-332 of mthAK

221   have been proposed to bind to the β-phosphate, α-phosphate, and adenine base of

222   ADP, respectively, although this has not been confirmed experimentally (Fig. 3)

223   (8). Ala-330 is located close to the β-phosphate and Asn-335 interacts with the

224   adenine base of ADP (Table S1), suggesting that Ala-330 and Asn-335 are key

225   residues in recognition of ATP in mthAK (Fig. 3). Superposition of the

226   substrate-binding site of the tertiary structure of mthAK complexed with acetate

227   and ADP-AlF$_3$ (9) and that of PPi-ehiAK (17) showed that the corresponding 5

228 residues in PPi-ehiAK would occlude the ATP-binding cleft of mthAK and thus

229 could reject binding of ATP to PPi-ehiAK (Fig. 3). Consistent with this

230 observation, Gln-323 and Met-324 of PPi-ehiAK have previously been proposed

231 to occlude the ATP-binding cleft (17).

232

233 **Kinetic analyses of variant ATP-ecoAKs**   The candidate residues in

234 mthAK/ATP-ecoAK/PPi-ehiAK   are   Asn-211/Asn-213/Thr-201,

235 Ala-330/Gly-332/Asp-322, Gly-331/Gly-333/Gln-323, Ile-332/Ile-334/Met-324,

236 and Asn-335/Asn-337/Glu-327 (Figs. 2 and 3). To examine the roles of these

237 residues in phosphoryl donor specificity, each candidate residue in ATP-ecoAK,

238 which is specific for ATP (Table 1), was substituted with the respective PPi-ehiAK

239 residue and the variant ATP-ecoAKs were purified (Fig. S2). All 5 variant

240 ATP-ecoAKs exhibited increased K_m and decreased V_{max} for ATP (Table 1),

241 indicating that these residues are the determinants for the specificity to ATP in

242 ATP-ecoAK. Notably, K_m for ATP of ATP-ecoAK N337E increased 46-fold

243 relative to ATP-ecoAK, showing a critical role of ATP-ecoAK Asn-337 in ATP

244 binding. Thus, Glu-327 of PPi-ehiAK may be a particularly potent determinant of

245 rejection of ATP and promotion of PPi specificity in PPi-ehiAK (Fig. 3, Table 1).

246 Each variant ATP-ecoAK showed no PPi-dependent AK activity for both acetyl

247 phosphate and PPi formation (Tables 1 and S2).

248

249 **Analyses of substrate binding to AKs**   Affinities of PPi-ehiAK, ATP-ecoAK,

250 and variant ATP-ecoAKs for each ATP and PPi were analyzed using DSF based on

251 changes in protein stability upon ligand binding (23). The fluorescence of SYPRO

252 Orange bound to denatured proteins was measured during heat treatment from 25

253 to 95°C. T_m values of AKs in the absence and presence of substrates were

254 determined as the midpoint of the increase in the fluorescence profile (Table 2).

255 The difference in T_m of native ATP-ecoAK in the presence and absence of ATP

256 ($\Delta T_{m\ ATP}$) was 13°C, suggesting that the thermal stability of ATP-ecoAK was

257 increased by the binding of ATP. In contrast, $\Delta T_{m\ ATP}$ of PPi-ehiAK could not be

258 measured, concordant with the absence of ATP-dependent activity of PPi-ehiAK

259 (Table 1). $\Delta T_{m\ ATP}$ of all variant ATP-ecoAKs was decreased significantly relative

260 to that of native ATP-ecoAK, in agreement with the decreased activity of variant

261 ATP-ecoAK and supporting the roles of the 5 residues as determinants of

262 specificity for ATP. The reason for the greatly decreased $\Delta T_{m\ ATP}$ for ATP-ecoAK

263 G332D remains to be clarified.

264　　To confirm the ATP-binding data, ATP-ecoAK, ATP-ecoAK N337E, and

265 PPi-ehiAK were added to an ATP-agarose column, washed, and eluted with 50

266 mM ATP containing 10 mM $MgCl_2$. As expected, ATP-ecoAK was eluted by ATP

267 after complete washing, while PPi-ehiAK was not eluted (Fig. S3), in agreement

268 with the absence of ATP-dependent activity of PPi-ehiAK and the DSF results

269 (Tables 1 and 2). Slight elution occurred for ATP-ecoAK N337E (Fig. S3), which

270 had a significantly increased K_m for ATP (Table 1). This confirms that the affinity

271 of ATP-ecoAK N337E for ATP was decreased by substitution of Asn-337 to Glu.

272　　$\Delta T_{m\ PPi}$ of PPi-ehiAK was 1.7, indicating the expected binding of PPi to

273 PPi-ehiAK (Table 2). Unexpectedly, $\Delta T_{m\ PPi}$ of ATP-ecoAK was 4.4, suggesting

274 that PPi can bind to ATP-ecoAK, although ATP-ecoAK cannot utilize PPi as a

275 phosphoryl donor for catalysis (Table 1). $\Delta T_{m\ PPi}$ of ATP-ecoAK was not markedly

276 reduced upon substitution of each candidate residue, especially Gly-333, Ile-334,

277 and Asn-337, compared to the effects on $\Delta T_{m\,ATP}$ (Table 2). This may reflect the

278 role of these residues in binding to adenosine of ADP, and thus not to PPi (Fig. 3).

279 Substitution of Asn-213 or Gly-332 of ATP-ecoAK reduced $\Delta T_{m\,PPi}$ of

280 ATP-ecoAK. This is in agreement with the putative binding of Asn-213 of

281 ATP-ecoAK to the ß-phosphate of ADP and putative equivalent binding of

282 Asn-211 of mthAK to the PPi moiety. Gly-322 of ATP-ecoAK is located close to

283 the ß-phosphate of ADP, and Ala-330 of mthAK may similarly be located close to

284 PPi (Fig. 3).

285 Asn-213 and Gly-332 of ATP-ecoAK correspond to Thr-201 and Asp-322 of

286 PPi-ehiAK respectively (Figs. 2 and 3). To examine the involvement of Thr-201

287 and Asp-322 of PPi-ehiAK in utilization of PPi, we focused on the residues

288 (Leu-326 and Asn-376) of PPi-ehiAK that interact with Thr-201 and Asp-322

289 (Table S3, Fig. S4). Leu-326 and Asn-376 of PPi-ehiAK correspond to Glu-336

290 and Thr-385 of ATP-ecoAK. Glu-336, Thr-385, Asn-213 and Gly-332 of

291 ATP-ecoAK were substituted with the respective PPi-ehiAK residues (Leu-326,

292 Asn-376, Thr-201, and Asp-322) to give a quadruple ATP-ecoAK variant

293 (ATP-ecoAK N213T G332D E336L T385N) that had the possibility of utilizing

294 PPi (Fig. S2). However, this variant could not utilize PPi and $\Delta T_{m\,PPi}$ was not

295 increased by these substitutions. V_{max} and k_{cat} for ATP were significantly decreased

296 in the quadruple variant (Table 1) and $\Delta T_{m\,ATP}$ was markedly decreased (Table 2).

297

298 **DISCUSSION**

299

300　　　The results of the study show that PPi-ehiAK is specific for PPi and does not

301　　　utilize ATP (16), while ATP-ecoAK is specific for ATP and does not use PPi.

302　　　Based on the tertiary and primary structures and catalytic and binding activities of

303　　　variant enzymes, we identified 5 residues (Asn-213, Gly-332, Gly-333, Ile-334,

304　　　and Asn-337 in ATP-ecoAK) as determinants of specificity to ATP in ATP-ecoAK.

305　　　　ATP-ecoAK N337E exhibited a 46-fold increase in K_m for ATP relative to

306　　　ATP-ecoAK, indicating that Asn-337 of ATP-ecoAK is the most crucial for the

307　　　specificity to ATP and suggesting that the corresponding Asn-335 in mthAK is

308　　　also crucial for binding to ATP and that the corresponding Glu-327 in PPi-ehiAK

309　　　is possibly important for rejection of ATP in PPi-ehiAK. The basis of the role of

310　　　Asn-337 of ATP-ecoAK in accepting ATP was examined using molecular and

311　　　electrostatic surfaces of the ADP-binding sites of mthAK N335E and mthAK, for

312　　　which a tertiary structure has been solved (9). The ADP-binding cleft is negatively

313　　　charged in mthAK N335E, but positively charged in mthAK (Fig. S5). There was

314　　　no clear structural change in the molecular surface of mthAK N335E that could

315　　　have resulted in rejection of ATP. Thus, the negatively charged ATP-binding site

316　　　in ATP-ecoAK N337E may explain the weaker affinity for ATP.

317　　　　To get further insight into the substrate specificity of AKs, we examined how

318　　　the 5 key residues are distributed in the primary structures of AKs. A total of

319　　　2,625 proteins homologous to PPi-ehiAK from all species with sequenced

320　　　genomes were found using BLASTP (25). Among the homologs, the 5 key

321　　　residues　　of　　mthAK/ATP-ecoAK/PPi-ehiAK　　(Asn-211/Asn-213/Thr-201,

322　　　Ala-330/Gly-332/Asp-322, Gly-331/Gly-333/Gln-323, Ile-332/Ile-334/Met-324,

323　　　and Asn-335/Asn-337/Glu-327) are highly conserved as Asn, Ala or Gly, Gly, Ile,

324 and Asn, respectively (Table 3). These are mthAK- and ATP-ecoAK-specific

325 residues, which suggests that almost all organisms have ATP-dependent AKs. In

326 contrast, 10 PPi-ehiAK homologs, including PPi-ehiAK, possess the

327 PPi-ehiAK-specific residue (Glu) in the most crucial position determining the

328 phosphoryl donor specificity (corresponding to Asn-335/Asn-337/Glu-327 in

329 mthAK/ATP-ecoAK/PPi-ehiAK) (Table 3). However, except for PPi-ehiAK and

330 the PPi-ehiAK homolog from *Entamoeba dispar*, which is closely related to *E.*

331 *histolytica*, 8 of these homologs have no PPi-ehiAK-specific residues in the other

332 4 positions (corresponding to Thr-201, Asp-322, Gln-323, and Met-324 in

333 PPi-ehiAK) (Table S4). This suggests that only the PPi-ehiAK homolog from *E.*

334 *dispar* is PPi-dependent. The phosphoryl donor specificities of the other 8

335 PPi-ehiAK homologs remain to be clarified.

336

341

REFERENCES

1. **Thauer, R. K., Moller-Zinkhan, D., and Spormann, A. M.:** Biochemistry of acetate catabolism in anaerobic chemotrophic bacteria, Annu. Rev. Microbiol., **43**, 43-67 (1989).

2. **Rose, I. A.:** Acetate kinase of bacteria (acetokinase), Methods. Enzymol., **1**, 591-595 (1955).

3. **Matsuyama, A., Yamamoto, H., and Nakano, E.:** Cloning, expression, and nucleotide sequence of the *Escherichia coli* K-12 *ackA* gene, J. Bacteriol., **171**, 577-580 (1989).

4. **Knorr, R., Ehrmann, M. A., and Vogel, R. F.:** Cloning, expression, and characterization of acetate kinase from *Lactobacillus sanfranciscensis*, Microbiol. Res., **156**, 267-277 (2001).

5. **Aceti, D. J., and Ferry, J. G.:** Purification and characterization of acetate kinase from acetate-grown *Methanosarcina thermophila*. Evidence for regulation of synthesis, J. Biol. Chem., **263**, 15444-15448 (1988).

6. **Bock, A. K., Glasemacher, J., Schmidt, R., and Schonheit, P.:** Purification and characterization of two extremely thermostable enzymes, phosphate acetyltransferase and acetate kinase, from the hyperthermophilic eubacterium *Thermotoga maritima*, J. Bacteriol., **181**, 1861-1867 (1999).

7. **Fox, D. K., and Roseman, S.:** Isolation and characterization of homogeneous acetate kinase from *Salmonella typhimurium* and *Escherichia coli*, J. Biol. Chem., **261**, 13487-13497 (1986).

16

366   8.   **Buss, K. A., Cooper, D. R., Ingram-Smith, C., Ferry, J. G., Sanders, D.**

367   **A., and Hasson, M. S.:** Urkinase: Structure of acetate kinase, a member of

368   the ASKHA superfamily of phosphotransferases, J. Bacteriol., **183**,

369   680-686 (2001).

370   9.   **Gorrell, A., Lawrence, S. H., and Ferry, J. G.:** Structural and kinetic

371   analyses of arginine residues in the active site of the acetate kinase from

372   *Methanosarcina thermophila*, J. Biol. Chem., **280**, 10731-10742 (2005).

373   10.   **Ingram-Smith, C., Barber, R. D., and Ferry, J. G.:** The role of

374   histidines in the acetate kinase from *Methanosarcina thermophila*, J. Biol.

375   Chem., **275**, 33765-33770 (2000).

376   11.   **Ingram-Smith, C., Gorrell, A., Lawrence, S. H., Iyer, P., Smith, K.,**

377   **and Ferry, J. G.:** Characterization of the acetate binding pocket in the

378   *Methanosarcina thermophila* acetate kinase, J. Bacteriol., **187**, 2386-2394

379   (2005).

380   12.   **Miles, R. D., Iyer, P. P., and Ferry, J. G.:** Site-directed mutational

381   analysis of active site residues in the acetate kinase from *Methanosarcina*

382   *thermophila*, J. Biol. Chem., **276**, 45059-45064 (2001).

383   13.   **Miles, R. D., Gorrell, A., and Ferry, J. G.:** Evidence for a transition state

384   analog, MgADP-aluminum fluoride-acetate, in acetate kinase from

385   *Methanosarcina thermophila*, J. Biol. Chem., **277**, 22547-22552 (2002).

386   14.   **Singh-Wissmann, K., Ingram-Smith, C., Miles, R. D., and Ferry, J. G.:**

387   Identification of essential glutamates in the acetate kinase from

388   *Methanosarcina thermophila*, J. Bacteriol., **180**, 1129-1134 (1998).

389   15.   **Singh-Wissmann, K., Miles, R. D., Ingram-Smith, C., and Ferry, J. G.:**

390   Identification of essential arginines in the acetate kinase from

391   *Methanosarcina thermophila*, Biochemistry (Mosc). **39**, 3671-3677

392   (2000).

393   16.   **Fowler, M. L., Ingram-Smith, C., and Smith, K. S.:** Novel

394   pyrophosphate-forming acetate kinase from the protist *Entamoeba*

395   *histolytica*, Eukaryot. Cell, **11**, 1249-1256 (2012).

396   17.   **Thaker, T. M., Tanabe, M., Fowler, M. L., Preininger, A. M.,**

397   **Ingram-Smith, C., Smith, K. S., and Iverson, T. M.:** Crystal structures

398   of acetate kinases from the eukaryotic pathogens *Entamoeba histolytica*

399   and *Cryptococcus neoformans*, J. Struct. Biol., **181**, 185-189 (2013).

400   18.   **Kitagawa, M., Ara, T., Arifuzzaman, M., Ioka-Nakamichi, T., Inamoto,**

401   **E., Toyonaga, H., and Mori, H.:** Complete set of ORF clones of

402   *Escherichia coli* ASKA library (a complete set of *E. coli* K-12 ORF

403   archive): unique resources for biological research, DNA Res., **12**, 291-299

404   (2005).

405   19.   **Lipmann, F., and Tuttle, L. C.:** A specific micromethod for the

406   determination of acyl phosphates, J. Biol. Chem., **159**, 21-28 (1945).

407   20.   **Ghetta, A., Matus-Ortega, M., Garcia-Mena, J., Deho, G., Tortora, P.,**

408   **and Regonesi, M. E.:** Polynucleotide phosphorylase-based photometric

409   assay for inorganic phosphate, Anal. Biochem., **327**, 209-214 (2004).

410   21.   **Eriksson, J., Karamohamed, S., and Nyren, P.:** Method for real-time

411   detection of inorganic pyrophosphatase activity, Anal. Biochem., **293**,

412   67-70 (2001).

413   22.   **Bradford, M. M.:** Rapid and sensitive method for quantitation of

microgram quantities of protein utilizing principle of protein-dye binding, Anal. Biochem., **72**, 248-254 (1976).

23. **Niesen, F. H., Berglund, H., and Vedadi, M.:** The use of differential scanning fluorimetry to detect ligand interactions that promote protein stability, Nat. Protoc., **2**, 2212-2221 (2007).

24. **Laemmli, U. K.:** Cleavage of structural proteins during the assembly of the head of bacteriophage T4, Nature, **227**, 680-685 (1970).

25. **Altschul, S. F., Madden, T. L., Schaffer, A. A., Zhang, J., Zhang, Z., Miller, W., and Lipman, D. J.:** Gapped BLAST and PSI-BLAST: a new generation of protein database search programs, Nucleic. Acids. Res., **25**, 3389-3402 (1997).

26. **Kaminuma, E., Mashima, J., Kodama, Y., Gojobori, T., Ogasawara, O., Okubo, K., Takagi, T., and Nakamura, Y.:** DDBJ launches a new archive database with analytical tools for next-generation sequence data, Nucleic. Acids. Res., **38**, D33-38 (2010).

431 **FIGURES**

432
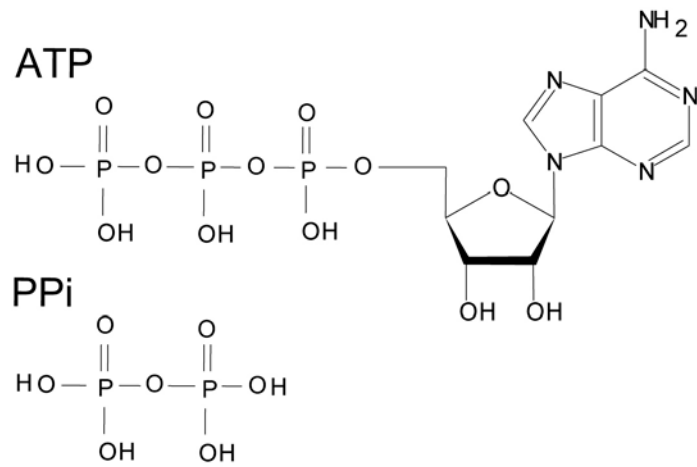
433

434 **Fig. 1.** Structures of ATP and PPi.

435

```
               7
mthAK     ---MKVLVINAGSSSLKYQLIDMTNESALAVGLCERIGIDNSIITQKKFDGKKLEKLTDL 57
ATP-ecoAK MSSKLVLVLNCGSSSLKFAIIDAVNGEEYLSGLAECFHLPEARIKWKMDGNKQEAALGAG 60
PPi-ehiAK --MSNVLIFNVGSSSLTYKVFCSDNIVCSGKSNRVNVTGTEKPFIEHHLNGQIIKIETPI 58
           **:* ***** : :: *    .    : : : ..:
                                           91
mthAK     PTHKDALEEVVKALTDDEFGVIKDMGEINAVGHRVVHGGEKFTTSALYDEGVEKAIKDCF 117
ATP-ecoAK AAHSEALNFIVNTILAQKP---ELSAQLTAIGHRIVHGGEKYTSSVVIDESVIQGIKDAA 117
PPi-ehiAK LNHPQAAKLIIQFLKENHIS-------IAFVGHRFVHGGSYFKKSAVIDEVVLKELKECL 111
           * :* : ::: : :.        : :***.****. :..*. : ** * : :*:.
                               148
mthAK     ELAPLHNPPNMMGISACAEIMPGTP--MVIVFDTAFHQTMPPYAYMYALPYDLYEKHGVR 175
ATP-ecoAK SFAPLHNPAHLIGIEEALKSFPQLKDKNVAVFDTAFHQTMPEESYLYALPYNLYKEHGIR 177
PPi-ehiAK PLAPIHNPSSFGVIEISMKELPTTR--QYVAIDTAFHSTISQAERTYAIPQPYQSQY--L 167
           :**:***. : *. . : :*    .:*****.*:. **:*   .::
            180                       211
mthAK     KYGFHGTSHKYVAERAALMLGKPAEETKIITCHLGNGSS-ITAVEGGKSVETSMGFTPLE 234
ATP-ecoAK RYGAHGTSHFYVTQEAAKMLNKPVEELNIITCHLGNGGS-VSAIRNGKCVDTSMGLTPLE 236
PPi-ehiAK KFGFHGLSYEYVINSLKNVID--VSHSKIIACHLGTGGSSCCGIVNGKSFDTSMGNSTLA 225
           ::* ** *: **  :    ::. ...  :**:****.*.* .:.**..:**** :.*
            241
mthAK     GLAMGTRCGSIDPAIVPFLMEKEGLTTREIDTLMNKKSGVLGVSGLSNDFRDLDEAASKG 294
ATP-ecoAK GLVMGTRSGDIDPAIIFHLHDTLGMSVDAINKLLTKESGLLGLTEVTSDCRYVEDNYAT- 295
PPi-ehiAK GLVMSTRCGDIDPTIPIDMIQQVG--IEKVVDILNKKSGLLGVSELSSDMRDILHEIETR 283
           **.*.**.*.***:*   : : *     : :.*:**:**:: ::.* * :.   .
                                        330 331 332 335
mthAK     ---NRKAELALEIFAYKVKKFIGEYSAVLNG-ADAVVFTAGIGENSASIRKRILTGLDGI 350
ATP-ecoAK ---KEDAKRAMDVYCHRLAKYIGAYTALMDGRLDAVVFTGGIGENAAMVRELSLGKLGVL 352
PPi-ehiAK GPKAKTCQLAFDVYIKQLAKTIGGLMVEIGG-LDLLVFTDQMGLEVWQVRKAICDKMKFL 342
           . .: *:::: :: * ** . .:* * :*** :*: :*:   : :
                                 384
mthAK     GIKIDDEKN-KIRGQEIDISTP-DAKVRVFVIPTNEELAIARETKEIVETEVKLRSSIPV 408
ATP-ecoAK GFEVDHERNLAARFGKSGFINK-EGTRPAVVIPTNEELVIAQDASRLTA---------- 400
PPi-ehiAK GIELDDSLNEKSMGKKIEFLTMPSSKVQVCVAPNDEELVILQKGKELFQF---------- 392
           *::.*.. *   : :.  ... . * *.:***.* :. ..:
```

436

Fig. 2. Multiple alignment of the primary sequences of mthAK, ATP-ecoAK, and

PPi-ehiAK. Multiple alignment of the mthAK (Uniprot, P38502), ATP-ecoAK

(KEGG, Y75_p2262), and PPi-ehiAK (KEGG, EHI_170010) sequences was

conducted using ClustalW2 (26). The 12 residues located within 4.0 Å of ADP in

the tertiary structure of mthAK complexed with acetate and ADP-AlF$_3$ (9) are

shown in bold. Among these 12 residues, the 5 candidate residues for

determination of phosphoryl donor specificity are denoted by arrowheads. Key

residues involved in catalysis in mthAK (Asn-7, Arg-91, Asp-148, His-180,

Arg-241, and Glu-384) (8-10) are conserved in ATP-ecoAK and PPi-ehiAK and

21

are boxed. Identical residues are denoted by an asterisk (*), strongly conserved

447 residues by a colon (:), and weakly conserved residues by a period (.). Numbers

448 above the sequences refer to mthAK and numbering for each protein is shown on

449 the right.

450

451

452

453
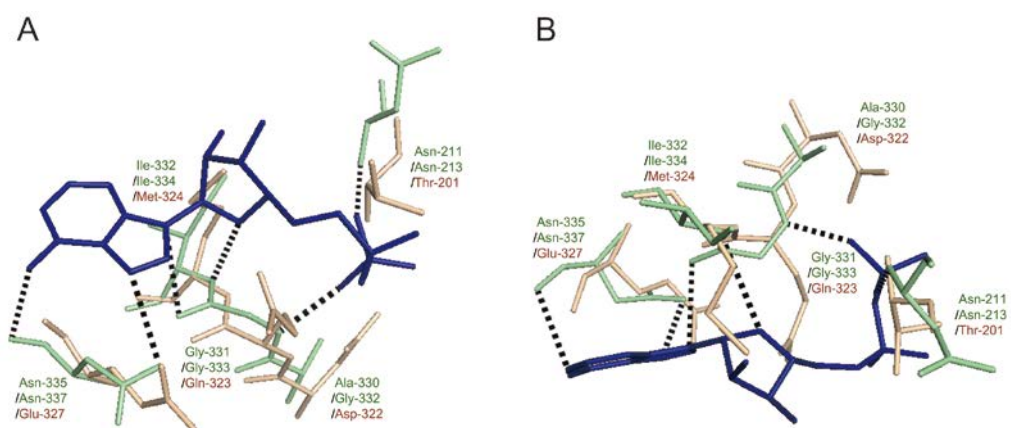
Fig. 3. Superposition of the substrate-binding site structures of mthAK and

PPi-ehiAK. A, Superposition of the substrate-binding sites of PPi-ehiAK (PDB,

4H0O) (17) and mthAK complexed with acetate and ADP-AlF$_3$ (PDB, 1TUY) (9).

Amino acid residues of mthAK are shown in green, ADP in mthAK is in deep

blue, and PPi-ehiAK is in light orange. Residue names and numbers are shown as

mthAK (green)/ATP-ecoAK (green)/PPi-ehiAK (pink). Hydrogen bonds in

mthAK are shown as dashed lines. B, Overhead view of *A*. Superposition of AKs

was performed using PyMOL.

Table 1. Kinetic constants of AKs.[a]

Phosphoryl donor	PPi			ATP		
	K_m (mM)	V_{max} (U/mg)	k_{cat} (s^{-1})	K_m (mM)	V_{max} (U/mg)	k_{cat} (s^{-1})
PPi-ehiAK	3.3 ± 0.5	3.7 ± 0.2	2.6 ± 0.1	nd	nd	nd
ATP-ecoAK	nd [b]	nd	nd	0.67 ± 0.06	1258 ± 28	908 ± 20
ATP-ecoAK N213T	nd	nd	nd	1.7 ± 0.2	22.7 ± 1.1	16.3 ± 0.8
ATP-ecoAK G332D	nd	nd	nd	3.5 ± 0.4	13.7 ± 0.7	9.9 ± 0.5
ATP-ecoAK G333Q	nd	nd	nd	5.2 ± 0.4	56.8 ± 1.5	41.0 ± 1.1
ATP-ecoAK I334M	nd	nd	nd	6.6 ± 0.6	72.8 ± 3.3	10.5 ± 0.5
ATP-ecoAK N337E	nd	nd	nd	30.7 ± 1.9	537 ± 24	395 ± 18
ATP-ecoAK N213T G332D E336L T385N	nd	nd	nd	0.66 ± 0.18	0.47 ± 0.01	0.34 ± 0.01
PPi-ehiAK [c]	3.6 ± 0.1	nr	nr	nr	nr	nr
ATP-ecoAK [d]	nr	nr	nr	0.07	2,000	nr

[a] AK activity was assayed with different concentrations of PPi or ATP. nd, not detected. nr, not reported. Kinetic values were calculated by fitting data to the appropriate Michaelis-Menten equations using KaleidaGraph software (Synergy Software). [b] ΔA_{540} was 0.11 in the presence of 5 mM PPi with 15.8 µg of PPi-ehiAK after a 10 min reaction, but ΔA_{540} was zero in the presence of 10 mM PPi with 20 µg of ATP-ecoAK, ATP-ecoAK N213T, ATP-ecoAK G332D, ATP-ecoAK G333Q, ATP-ecoAK I334M and ATP-ecoAK N337E after 10, 30 and

60 min; thus AK activities of ATP-ecoAK and variant ATP-ecoAK toward PPi were regarded as not detected (nd). ΔA_{540} was 0.036 in the presence of 10 mM ATP with 6.4×10^{-3} µg of ATP-ecoAK after a 10 min reaction, but ΔA_{540} was zero in the presence of 5 mM ATP with 15.8 µg of PPi-ehiAK after 10, 30 and 60 min; thus AK activities of PPi-ehiAK toward ATP were regarded as not detected. [c] Data from a previous report (16). [d] Data from a previous report (7).

Table 2. Differences in T_m of AKs in the absence and presence of ATP and PPi.

Enzyme	$\Delta T_{m\,ATP}$ (°C)	$\Delta T_{m\,PPi}$ (°C)
PPi-ehiAK	nd	1.7 ± 0.2
ATP-ecoAK	12.5 ± 0.9	4.4 ± 0.6
ATP-ecoAK N213T	1.9 ± 0.1	1.7 ± 0.6
ATP-ecoAK G332D	0.22 ± 0.18	2.0 ± 0.1
ATP-ecoAK G333Q	2.7 ± 0.1	3.7 ± 0.2
ATP-ecoAK I334M	1.3 ± 0.2	3.3 ± 0.2
ATP-ecoAK N337E	1.0 ± 0.1	3.4 ± 0.3
ATP-ecoAK N213T G332D E338L T385N	0.73 ± 0.20	2.7 ± 0.2

Differences in T_m of AKs in the absence and presence of ATP and PPi ($\Delta T_{m\,ATP}$ and $\Delta T_{m\,PPi}$) are shown. ATP was used at 1.0 mM and PPi at 5.0 mM. Means and standard deviations of three independent experiments are shown. nd, not detected.

Table 3. Distribution of the 5 candidate residues in AK sequences in a database search.[a]

Candidate residues of mthAK/ATP-ecoAK/PPi-ehiAK	mthAK/ATP-ecoAK-specific residues	PPi-ehiAK-specific residues
Asn-211/Asn-213/Thr-201	Asn (2,100/80%) [b]	Thr (2/0.08%)
Ala-330/Gly-332/Asp-322	Ala or Gly (2,584/98%)	Asp (3/0.11%)
Gly-331/Gly-333/Gln-323	Gly (2,581/98%)	Gln (2/0.08%)
Ile-332/Ile-334/Met-324	Ile (1,752/67%)	Met (78/3%)
Asn-335/Asn-337/Glu-327	Asn (2,101/80%)	Glu (10/0.38%)

[a] Distribution of the 5 candidate residues of mthAK/ATP-ecoAK/PPi-ehiAK (Asn-211/Asn-213/Thr-201, Ala-330/Gly-332/Asp-322, Gly-331/Gly-333/Gln-323, Ile-332/Ile-334/Met-324, and Asn-335/Asn-337/Glu-327) in a database search of AKs. A total of 2,625 PPi-ehiAK homologs were found using BLASTP (25) on the GenomeNet server (http://www.genome.jp). [b] Number and percentage (%) of PPi-ehiAK homologs possessing the indicated amino acid at the position of the candidate residue.

Supplementary information

Table S1. Interactions between mthAK and ADP [a]

	Hydrogen bonds			van der Waals contacts	
ADP atoms	Target atoms	Distance (Å)	ADP atoms	Target atoms	Distance (Å)
β-phosphate					
O2B	Asn-211[b] N	2.7			
O3B	Gly-331[b] N	2.6			
Ribose					
O2'	Phe-284[c] N	3.3	C1'	Gly-331[b] C	3.7
O3'	Asp-283[c] OD2	3.3		Ile-332[b] CG1	3.5
O4'	Ile-332[b] N	3.6	C2'	Phe-284[c] CB	3.9
Adenine					
N3	Arg-285[c] N	3.5	C2	Arg-285[c] CA	3.6
N6	Asn-335[b] O	3.4		CB	3.9
	Arg-362[d] NH$_2$	3.2		Ser-336[d] CB	3.8
N7	Asn-335[b] ND2	3.2	C5	Asn-335[b] CB	3.8
N9	Gly-331[b] O	3.4			

[a] Interactions between ADP and residues of mthAK B chain. [b] Five candidate residues specific to PPi-ehiAK. [c] Five residues conserved in mthAK, ATP-ecoAK, and PPi-ehiAK. [d] Residues not conserved.

Table S2. AK activity in the PPi-forming direction using Pi as a phosphoryl acceptor [a].

Enzyme	PPi (µM)
PPi-ehiAK	3.1
ATP-ecoAK	nd [b]
ATP-ecoAK N213T	nd
ATP-ecoAK G332D	nd
ATP-ecoAK G333Q	nd
ATP-ecoAK I334M	nd
ATP-ecoAK N337E	nd

[a] AK activity in the PPi-forming direction was assayed as described in the Materials and Methods. After reaction for 20 min with 1.4×10^{-2} µg of PPi-ehiAK, the reaction mixture was diluted 50-fold with distilled water and RLU was measured. PPi at 1.0 µM gave ΔRLU of 955,937. nd, not detected.

[b] ΔRLU was zero with 9.2, 3.1, 2.4, 5.8, 2.9, and 3.1 µg of ATP-ecoAK, ATP-ecoAK N213T, ATP-ecoAK G332D, ATP-ecoAK G333Q, ATP-ecoAK I334M and ATP-ecoAK N337E, respectively, after the reaction for 20 min; thus, AK activities in the PPi-forming direction of ATP-ecoAK and these mutated ATP-ecoAKs using PPi were regarded as not detected (nd).

Table S3. Residues interacting with Thr-201 and Asp-322 in PPi-ehiAK[a].

	Hydrogen bonds			van der Waals contacts			
	Target atoms		Distance (Å)		Target atoms		Distance (Å)
Thr-201							
O	Gly-202[b]	N	3.4				
Asp-322							
O	Leu-326[c]	N	3.4				
OD1	His-198[b]	ND1	3.3	CA	Asn-376[c]	CG	3.9
		NE2	2.3	CB	Leu-199[b]	C	3.4
OD2	Leu-199[b]	O	3.6		Gly-200[b]	CA	3.9
	Gly-200[b]	N	3.3	CG	Leu-199[b]	C	3.9
N	Asn-376[c]	OD1	3.1		Gly-200[b]	CA	3.4

[a] The residues interacting with Thr-201 and Asp-322 in PPi-ehiAK. Thr-201 and Asp-322 are expected to be around the phosphate group. [b] Four residues conserved in the primary structures of mthAK, ATP-ecoAK, and PPi-ehiAK. [c] Two residues conserved in ATP-dependent AKs, but not in PPi-ehiAK. This is the reason why we focused on these residues (Leu-326 and Asn-376 in PPi-ehiAK).

Table S4. Distribution of the 5 candidate residues.

Homolog name	Species name	Amino-acid residue corresponding to				
		Glu-327	Thr-201	Asp-322 of PPi-ehiAK	Gln-323	Met-324
EDI_237080 [a]	*Entamoeba dispar*	Glu	Thr	Asp	Gln	Met
GM21_0328 [a]	*Geobacter* sp. M21	Glu	Asn	Tyr	Gly	Glu
Gbem_0348 [a]	*Geobacter bemidjiensis*	Glu	Asn	Tyr	Gly	Glu
GM18_0425 [a]	*Geobacter* sp. M18	Glu	Asn	Tyr	Gly	Glu
Tpet_1041 [a]	*Thermotoga petrophila*	Glu	Ser	Gly	Gly	Met
Tnap_1061 [a]	*Thermotoga naphthophila*	Glu	Ser	Gly	Gly	Met
TRQ2_1071 [a]	*Thermotoga* sp. RQ2	Glu	Ser	Gly	Gly	Met
Tmari_1762 [a]	*Thermotoga maritima*	Glu	Ser	Gly	Gly	Met
TM1754 [a]	*Thermotoga maritima*	Glu	Ser	Gly	Gly	Met
ATP-ecoAK [a, b]	*E. coli*	Asn	Asn	Gly	Gly	Ile
mthAK	*M. thermophila*	Asn	Asn	Ala	Gly	Ile

[a] Proteins in KEGG database (http://www.genome.jp/kegg/).

[b] Y75_p2262 in KEGG database.

CGCGCGGCAGC<u>CAT**ATG**</u>TCTAATGTGCTGATTTTCAACGTAGGATCTAGTTCCCTCACATATAAA
GTGTTTTGTAGCGACAACATCGTCTGTAGTGGCAAATCCAATCGCGTGAATGTGACTGGTACTG
AGAAACCGTTTATCGAACATCACTTAAACGGCCAAATCATTAAGATAGAAACCCCAATCCTCAA
CCATCCACAGGCTGCAAAACTGATTATCCAGTTCCTGAAAGAGAACCACATCTCTATTGCCTTT
GTAGGCCATCGCTTTGTTCATGGCGGGTCTTACTTTAAGAAATCAGCCGTCATTGACGAAGTCG
TGCTGAAAGAACTGAAAGAATGCCTGCCTTTAGCGCCCATTCATAACCCGAGCTCTTTCGGAG
TTATCGAAATCTCGATGAAAGAACTGCCAACCACTCGTCAGTATGTGGCGATCGATACGGCGTT
CCATTCGACCATTTCCCAAGCTGAACGCACCTATGCGATTCCGCAGCCGTATCAATCGCAGTAT
CTGAAATTCGGCTTTCACGGCCTGTCATACGAATACGTGATCAACTCGTTGAAGAATGTCATTG
ACGTAAGTCACAGCAAAATCATTGCATGCCATCTTGGTACAGGTGGCTCCTCATGCTGCGGCAT
TGTGAATGGGAAATCGTTTGATACGAGTATGGGTAACAGCACACTTGCTGGTCTGGTGATGTCA
ACGCGTTGTGGGGATATTGATCCCACCATTCCGATTGATATGATCCAGCAAGTGGGTATTGAGA
AAGTTGTCGATATTCTCAACAAGAAAGCGGCTTGCTTGGGGTCAGTGAACTGAGCAGCGATA
TGCGCGATATTTTGCACGAAATCGAAACCCGTGGTCCTAAAGCCAAAACGTGCCAACTGGCCT
TTGATGTTTACATCAAACAGCTGGCGAAAACCATCGGAGGCCTGATGGTTGAGATCGGCGGTC
TTGACTTACTGGTGTTCACCGATCAGATGGGTCTGGAAGTATGGCAAGTTCGGAAAGCGATATG
CGACAAAATGAAATTTCTGGGCATTGAGTTGGACGATAGCCTCAATGAGAAGTCCATGGGTAA
GAAAATTGAATTCCTGACGATGCCGAGCAGCAAGGTACAGGTTTGTGTTGCACCGAATGACGA
GGAATTAGTCATACTGCAGAAAGGGAAGAATTATTCCAGTTT**TAA**<u>CTCGAG</u>CACCACCACC

Fig. S1. The sequence of *PPi-ehiAK* with optimized codon usage for *E. coli*. The optimized
PPi-ehiAK gene (KEGG ID; ehi: EHI_170010) was synthesized at Operon. The *Nde*I site
(CATATG) and *Xho*I site (CTCGAG) are underlined. The start codon (ATG) and stop codon
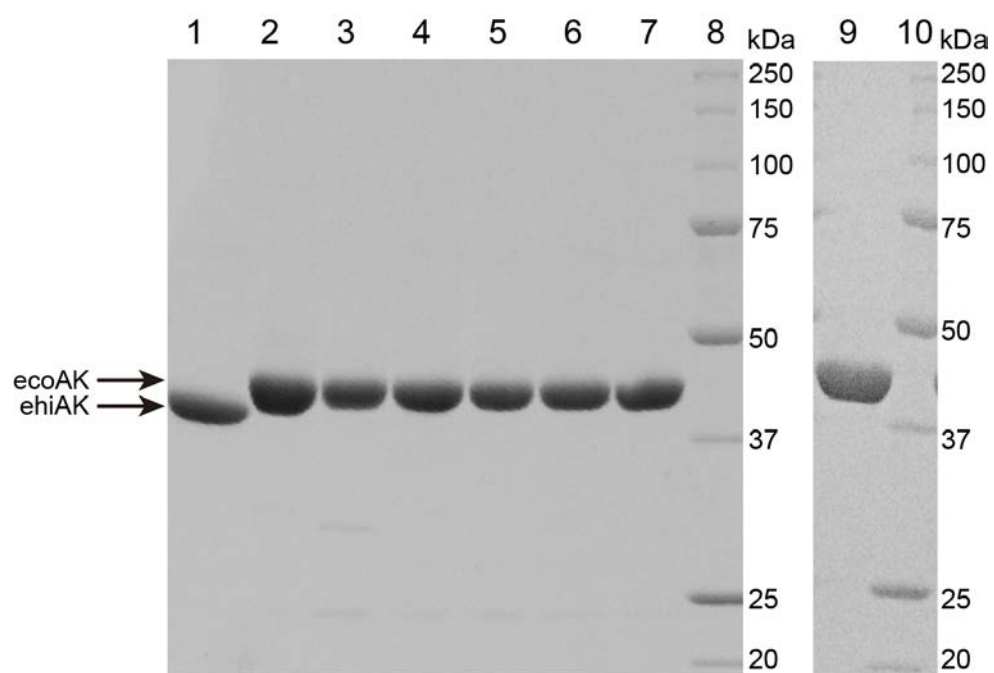(TAA) are shown in bold.

Fig. S2. SDS-PAGE of purified AKs. Lanes 1–7, 9: purified PPi-ehiAK, ATP-ecoAK, ATP-ecoAK N213T, ATP-ecoAK G332D, ATP-ecoAK G333Q, ATP-ecoAK I334M, ATP-ecoAK N337E, and ATP-ecoAK N213T G332D E336L T385N (5.0 μg). Arrows indicate positions of purified AKs. Lanes 8 and 10: protein markers (Bio-Rad Laboratories, Hercules, CA).
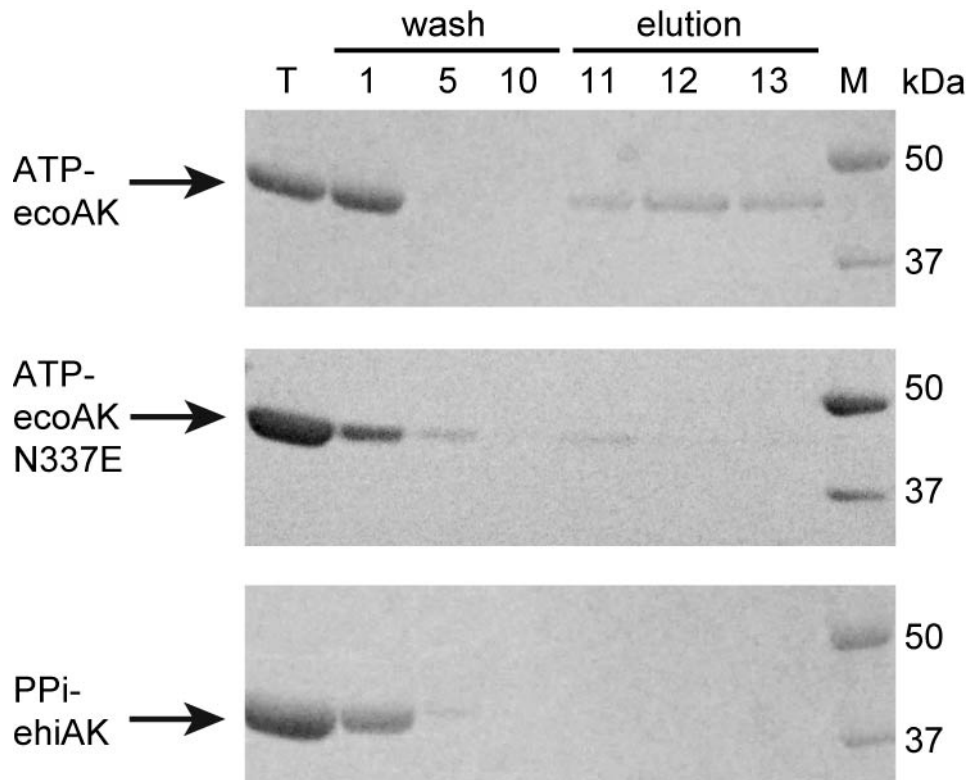
Fig. S3. SDS-PAGE of AKs eluted from an ATP-agarose column. Lane T: flow-through fraction; Lanes 1, 5, and 10: Fractions washed with 10 mM Tris-HCl (pH 8.0) containing 10 mM $MgCl_2$ or 20 mM HEPES-NaOH (pH 7.5) containing 10 mM $MgCl_2$; Lanes 11, 12, and 13: Fractions eluted with 50 mM ATP containing 10 mM $MgCl_2$; Lane M: protein markers. Lane numbers correspond to the numbers of fractions (200 µL each). Arrows indicate the positions of AKs.
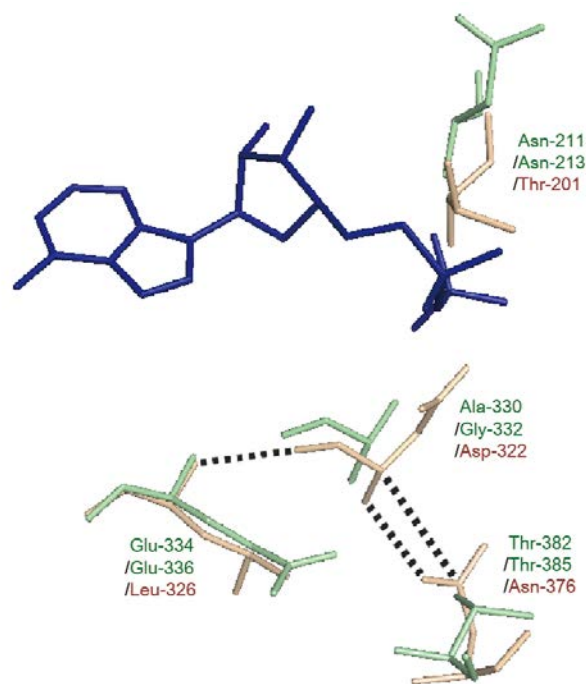
Fig. S4. Superposition of mthAK and PPi-ehiAK around the phosphate group of ADP. Superposition of the tertiary structure of PPi-ehiAK (PDB, 4H0O) (1) and that of mthAK complexed with acetate and ADP-AlF$_3$ (PDB, 1TUY) (2). Amino acid residues of mthAK are shown in green; ADP in mthAK is in deep blue, and PPi-ehiAK is in light orange. The residue names and numbers are shown for mthAK (green)/ATP-ecoAK (green)/PPi-ehiAK (pink). Hydrogen bonds in PPi-ehiAK are shown as dashed lines. Superposition of AKs was performed using PyMOL.
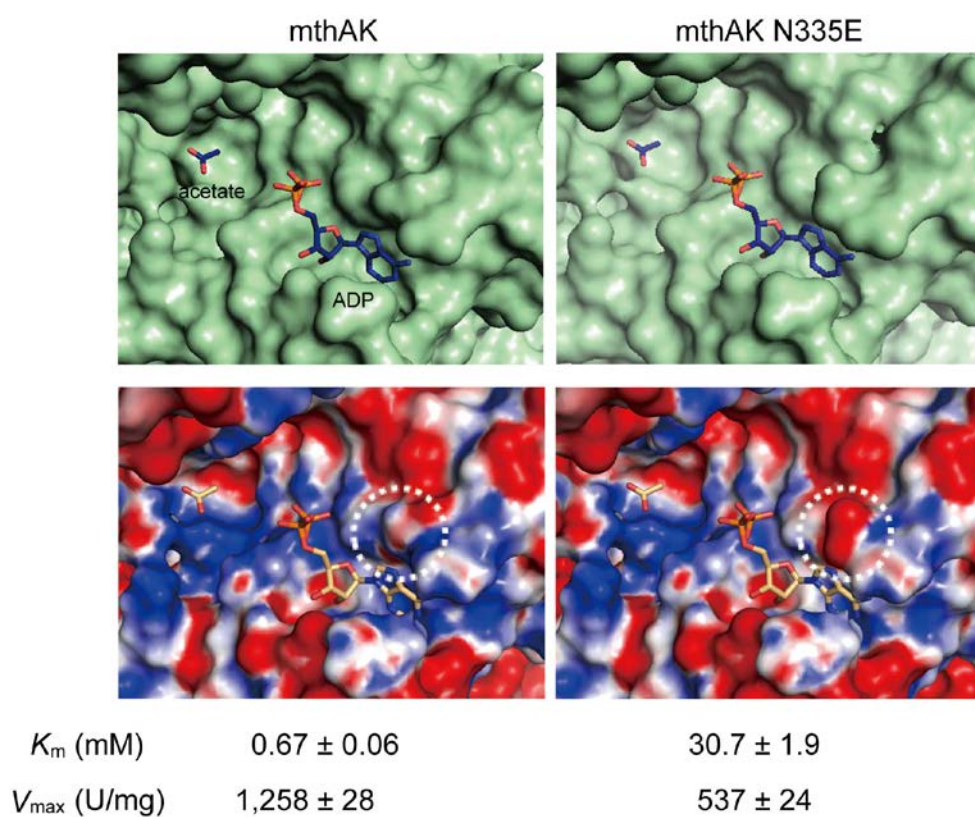
	mthAK	mthAK N335E
K_m (mM)	0.67 ± 0.06	30.7 ± 1.9
V_{max} (U/mg)	$1,258 \pm 28$	537 ± 24

Fig. S5. ADP-binding sites of mthAK and mthAK N335E. Molecular surfaces of ADP-binding sites of mthAK (left) and mthAK N335E (right) are shown in the upper panels. Electrostatic surfaces of the AKs are shown in the lower panels. Positive and negative charges at pH 7.0 are colored in blue and red, respectively, and were calculated using APBS (3). The position around Asn-335 is denoted by a white dotted circle. K_m and V_{max} for ATP of ATP-ecoAK and ATP-ecoAK N337E are shown under the respective figures.

References

1. **Thaker, T. M., Tanabe, M., Fowler, M. L., Preininger, A. M., Ingram-Smith, C., Smith, K. S., and Iverson, T. M.:** Crystal structures of acetate kinases from the eukaryotic pathogens *Entamoeba histolytica* and *Cryptococcus neoformans*, J. Struct. Biol., **181**, 185-189 (2013).

2. **Gorrell, A., Lawrence, S. H., and Ferry, J. G.:** Structural and kinetic analyses of arginine residues in the active site of the acetate kinase from *Methanosarcina thermophila*, J. Biol. Chem., **280**, 10731-10742 (2005).

3. **Baker, N. A., Sept, D., Joseph, S., Holst, M. J., and McCammon, J. A.:** Electrostatics of nanosystems: application to microtubules and the ribosome, Proc. Natl. Acad. Sci. USA., **98**, 10037-10041 (2001).